UV-A-Irradiated P(VDF-TrFE-CFE) as a High-Efficiency Refrigerant for Solid-State Cooling

Nouh Zeggai, Matthieu Fricaudet, Nicolas Guiblin, Brahim Dkhil, Martino Lobue, Morgan Almanza

UV-A irradiated P(VDF-TrFE-CFE) as a high efficiency refrigerant for solid-state cooling

Nouh Zeggai[*, a], *Matthieu Fricaudet* [b], *Nicolas Guiblin* [b], *Brahim Dkhil* [b], *Martino LoBue* [a], *Morgan Almanza* [*, a]

[a] Université Paris-Saclay, ENS Paris-Saclay, CNRS, SATIE, 91190 Gif-sur-Yvette, France

[b] Université Paris-Saclay, CentraleSupelec, CNRS, SPMS, 91190 Gif-sur-Yvette, France

Corresponding author: e-mail: nouh.zeggai@ens-paris-saclay.fr

Declarations of interest: none

Graphical abstract

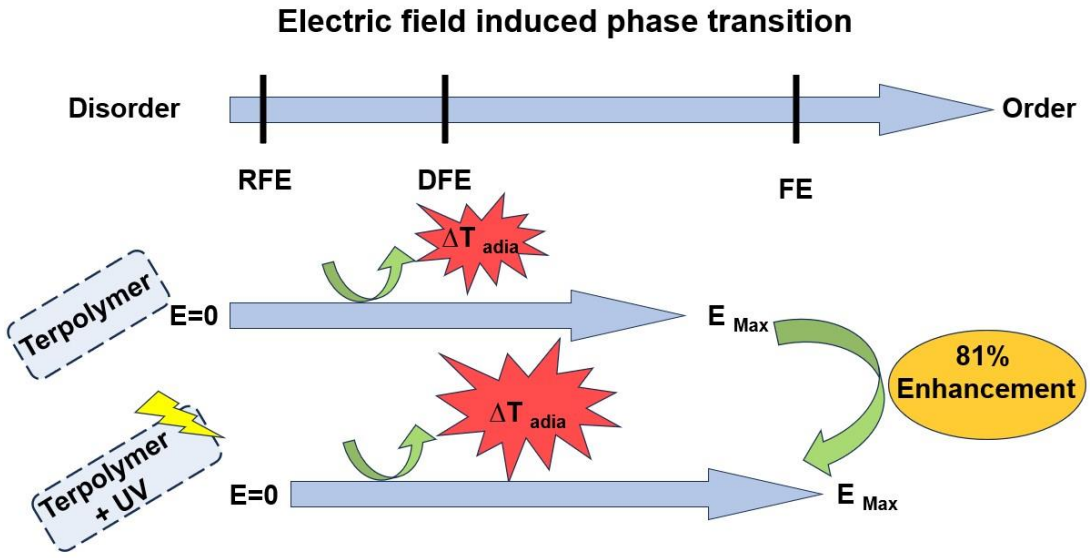

Abstract

Thin P(VDF-TrFE-CFE) films have become an essential active material in the manufacturing of solid-state refrigeration systems. Films prepared by solvent casting fall short of the performance needs of today's cooling devices due to their low electrocaloric (EC) response, 1.5 °C at 50 V/µm, and to their high dielectric losses. Here, we present a straightforward method for enhancing the EC effect and minimizing dielectric losses in P(VDF-TrFE-CFE) through low energy UV-A irradiation. This approach offers a potential path for post-improvement in the functional properties of EC materials. The material, after irradiation, shows new functional groups, thicker crystalline lamellae and denser structure. Direct measurements of the adiabatic temperature change have shown an increasing of the EC response from 1.76 °C to 2.88 °C at 60V/µm, accompanied by a reduction of the losses, two key improvements for potential applications. X-ray diffraction under electric field reveals an adiabatic temperature change related to the electric field induced appearance of the so-called defective ferroelectric (DFE) phase jointly with the ferroelectric (FE) one. After irradiation the FE phase appears at lower field, indicating that UV induced

modifications favor the polar phase. This work shows an easy to implement road towards properties enhancement of EC P(VDF-TrFE-CFE) films for cooling applications.

Keywords: Electrocaloric effect; P(VDF-TrFE-CFE); loss reduction; UV irradiation; Phase transition

I. Introduction

According to the International Energy Agency nearly 20% of the total electricity consumption in buildings around the world is used for cooling. The rising demand for space cooling associated with climate change is putting an enormous strain over the energy production infrastructures, driving a further increasing of emissions [1]. Between the solid-state alternatives to gas refrigerant for a new, more eco-friendly, generation of cooling technologies, electrocaloric materials attract a growing interest due to their outstanding caloric properties, and to the compactness of the associated field source [2–4]. Electrocaloric (EC) effect is the reversible temperature change of a ferroelectric material under the application of an electric field [5]. It is characterized by two main quantities that are measured under a field variation: the isothermal entropy change (ΔS) and the adiabatic temperature change (ΔT_{adia}). So far, several cooling devices based on EC effect have been developed [3,6]. One of the most promising candidates as an EC refrigerant is the P(VDF-TrFE-CFE) terpolymer (P, poly; VDF, vinylidene fluoride; TrFE, trifluoroethylene; CFE, chlorofluoroethylene) due to its large adiabatic temperature change, and to the possibility to be easily processed into thin films (e.g.. solvent casting) [5]. However, to fit the high efficiency needs of the new generation of cooling devices, the EC effect in P(VDF-TrFE-CFE) needs to be improved increasing ΔT_{adia}, and keeping the associated losses as low as possible.

P(VDF-TrFE-CFE) is a semicrystaline polymer that belongs to the family of relaxor-ferroelectric (RFE). It exhibits strong electroactive properties. Namely, it is electrostrictive, pyroelectric, and electrocaloric and it shows high energy storage properties[7]. P(VDF-TrFE-CFE) is derived from PVDF, poly (vinylidene fluoride). PVDF crystalline part can exist in different polymorphism depending on the chain conformations, such as: the paraelectric (PE) phase tg^+tg^- (i.e. alpha phase), the ferroelectric (FE) phase all-*trans* (i.e. beta phase) or $tttg^+tttg^-$ (i.e. gamma phase). Here, t (*trans*) and g (*gauche*) refer to the torsional bond arrangements with substituents at 180° and 60° to each other respectively. To stabilize the phase with the highest polarization (all-*trans*), copolymerization of PVDF with TrFE is commonly used. P(VDF-TrFE) have the tendency to crystallize into a ferroelectric, mostly all–*trans,* conformation phase showing a ferroelectric to paraelectric transition at a given temperature (T_c), depending on the TrFE content [8,9]. Typically, T_c is comprised between 50°C and the melting temperature (T_m). The incorporation of a third monomer, such as CFE, expands the interplanar distance and weakens the interchain interaction of the ferroelectric phase, favoring the tg^+tg^- conformation [10]. In this case, CFE limits all-trans sequence length (reducing the number of consecutive trans conformations) and provides the pinning force for fast conformation/polarization reversal after removing the external electric field. By adjusting the amount of CFE, due to the weakening of the interchain interactions, T_c moves towards room temperature improving the electrocaloric response and with 66% mol TrFE, 9% mol CFE, the ferroelectric becomes a relaxor ferroelectric. The latter shows a hexagonal-like structure which is similar to the high-temperature paraelectric phase of P(VDF-TrFE) [10]. This is the composition used in this work. Below the temperature of the transition RFE to PE, P(VDF-TrFE-CFE) contains mostly t_mg ($m<4$) conformation, above T_c conformations gradually transform into shorter t sequences and the inter-planar

distance increase, indicating the formation of the PE phase [11]. On the contrary, under high electric fields, the ferroelectric phase (all-trans) is formed within the relaxor polymer [12]. This change of conformation associated to high entropy change and its extreme sensitivity to electric field and to the temperature, are the key features to achieve high EC effect.

Introducing defects is commonly considered a way to promote the conformational change driven by the electric field. In combination with the CFE, several methods have been reported to introduce defects improving the EC response. The most common are; the blending of P(VDF-TrFE) with P(VDF-TrFE-CFE) [13], Barium Ziconate Titanate , Barium Strontium Titanate, boron nitrate fibers (BNf) + BCZT@$BaTiO_3$ nanoparticles to form a nanocomposite [14–16]. More recently, chemical conversion of a small number of the chlorofluoroethylene groups into terpolymer by a covalent double bond has been reported as a promising defect creation route [12,17]. All the studies mentioned above enhance the EC effect through an increase in crystallinity accompanied by a decrease of the crystalline size. It has been suggested that dipoles may exhibit distinct responses depending on their location, either at the interface or within the crystal [18]. Dipole at the interface are less confined and therefore they are expected to be more susceptible to the electric field [18].

Irradiation is also a method to induce defects that entail a disordering of the structure. Several works reported the induction of structural changes in PVDF based polymers using various type of radiations including heavy ions [19], e-beam[20] ,γ (Gamma) [21,22], Ultraviolet (UV). For instance, high energy ions implantation on PVDF causes a dramatic effect on the concentrations of fluorine and hydrogen in the material and leads to the formation of carbon-carbon double bonds [19]. Likewise, high energy e-beam irradiation of P(VDF-TrFE) has been reported to create cross-linking and chain-scission reactions, resulting in a transition from ferroelectric (FE) to relaxor ferroelectric

(RFE) [20]. Furthermore, it has been shown that γ –irradiation can foster the presence of radicals with distinct structures, mobility, and stability, accompanied by intramolecular crosslinking [23]. Still, the main drawbacks associated with high-energy irradiation are undesirable degradations as, for instance, the resulting brittleness of the material.

Ultraviolet (UV) irradiation offers a less energy-intensive approach, easier to carry out, and allows high-throughput processing conditions such as roll-to-roll processing. UV irradiation has been used to change the structure of fluoropolymer through the cross-linking scission and the formation of a new bounds [23–26]. Indeed, C-C, C-H and C-F bond energies (i.e. 4.2 eV and 5 eV respectively) are below the energy range of UV-C, and V-UV (i.e. in the 4.43 - 12.4 eV interval). Nonetheless, low-energy UV-A irradiation, with wave lengths in the 340−400 nm interval, and energies in 3.1 - 3.9 eV interval, has been successfully used to change PVDF properties [26].

In this work, we study the effect of short (less than 20 min), standard irradiance (circa 0.5 W/cm^2), low energy UV-A (UV LED with a spectrum centered around 395 nm) irradiation, on the electrocaloric properties of P(VDF-TrFE-CFE) films. After irradiation an increase of ΔT_{adia} up to 2.88 °C at 60 V/µm is observed, amounting to an enhancement of 81% compared to pristine P(VDF-TrFE-CFE). To the best of our knowledge, the effect of ultraviolet irradiation on the EC response, and on dielectric losses has never been investigated on P(VDF-TrFE-CFE). This makes the findings presented here relevant for the enhancement of this ter-polymer in view of its application as a solid-state refrigerant.

To shed light on the mechanisms underlying the EC effect improvement through UV irradiation a setup designed to carry out a direct measurement of the adiabatic temperature has been used [27]. In addition, X-ray diffraction (XRD) performed under electric field, a non-standard technique, will be used to underpin the main mechanisms

responsible for the EC effect measured on the pristine, and on the irradiated samples. Thereupon a complex interplay between three different phases is revealed and discussed. Jointly with the EC response, the losses have been measured allowing estimating an upper bound for the relative cooling efficiency of the material when cycled in relevant operating conditions. An efficiency improvement from 1.3 % for the pristine material, up to 2.2% after UV irradiation has been extrapolated. A significant result indeed, considering that losses represent the main bottleneck towards the use of P(VDF-TrFE-CFE) films as refrigerant in actual cooling devices [27]. The main result here is demonstrating low energy UV-A irradiation as a straightforward and efficient method to foster EC effect response in P(VDF-TrFE-CFE).

The paper is organized as follows: after the introduction (section I), the main experimental results are presented and discussed in section II; Section III is devoted to the general conclusions, and to discussing the new perspectives the main results of this study are opening; Section IV gives a detailed description of the experimental methods.

II. Results and discussion

The adiabatic temperature change ΔT_{adia} is the temperature variation when the electric field is applied under adiabatic conditions. **Figure. 1** shows the evolution of the EC effect of pristine and irradiated (with irradiation times spanning from 5 min up to 20 min) terpolymer films measured at room temperature. Below 20 V/µm the irradiated and non-irradiated films show almost the same adiabatic temperature change ΔT_{adia}. The effect of UV-Irradiation appears above 20 V/µm with a trend that is independent from the irradiation time. At 60 V/µm the ΔT_{adia} increases up to 2.88°C, an 81% with respect to the pristine sample.

The lack of experimental standards for characterizing EC effect makes comparison with data from the literature somewhat problematic. On the contrary, the rather high relative improvement of the sample properties gives a self-contained assessment of the positive effect of UV-irradiation. Nonetheless, it is worth nothing that the adiabatic temperature change obtained after irradiation gets not very far from the highest electrocaloric performance hitherto reported. The results presented here reach a ΔT_{adia} slightly below the performance of the P(VDF-TrFE-CFE)/ P(VDF-TrFE) blend (ΔT_{adia} ~ 4.1 K)[28] and of the (PVDF-TrFE-CFE) modified by double bond [29]. In general, direct measurements on polymers and nanocomposites (with $E \leq 60$ V/μm), gives ΔT_{adia} ranging from 3 to 4.2 °C (refer to Table S1 in the supporting information).

To check the stability in time of the UV induced changes, an irradiated sample has been characterized just after irradiation, and three months later. No relevant changes have been observed on 5-min irradiated film (the only film remaining without breakdown) confirming the UV induced improvement as a permanent modification of the material (see supplementary Figure S8).

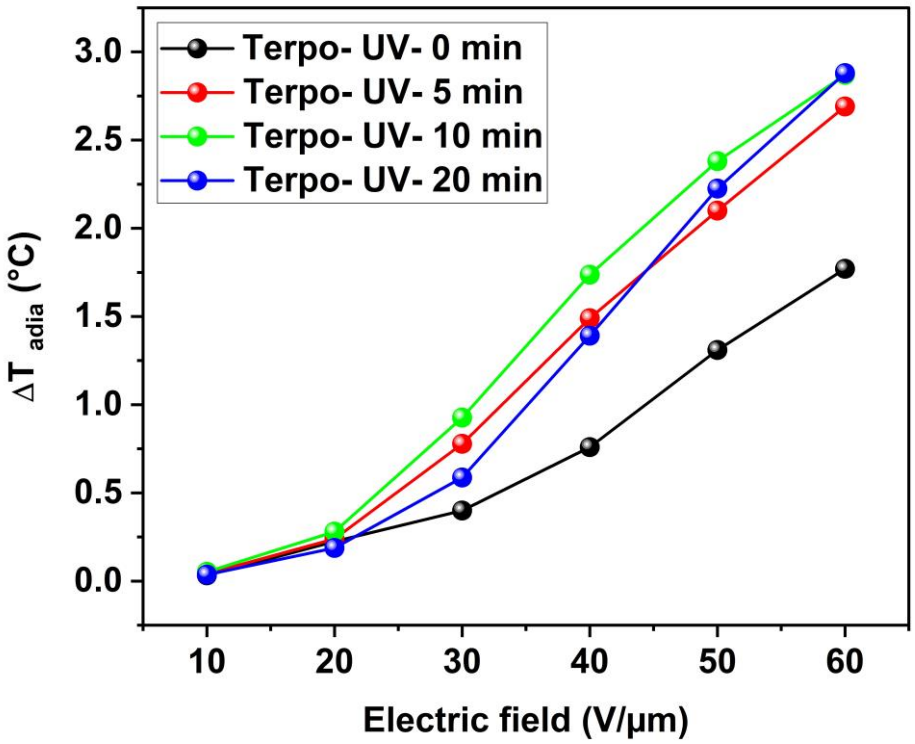

Figure. 1. The evolution of $\boldsymbol{\Delta T_{adia}}$ versus electric field for pristine and terpolymers irradiated at ambient temperature (25°C), under different irradiation times.

Building upon the methodology outlined in reference [27] , we have calculated the upper limit for the efficiency η of an optimal thermodynamic cycle that employs the materials studied here as refrigerants. By utilizing direct measurements of ΔT_{adia} and losses W_{loss} under unipolar square excitation (as shown in Error! Reference source not found.), we use an ideal thermodynamic cycle to extrapolate the upper bound of the efficiency using following expression:

$$\eta = \frac{1}{1-4TW_{loss}/c\Delta T^2{}_{adia}} \quad (1)$$

Where W_{loss} is the energy corresponding to the area of the P(E) loops, c is the volumetric heat capacity and ΔT_{adia} is the adiabatic temperature change. It is important

to highlight, that the unipolar excitation is better than the bipolar one because it provides the same ΔT_{adia} with less losses.

Figure. 2 presents the efficiency calculated from equation (2) for the pristine terpolymer and for the irradiated ones. Whereas, as shown in **Figure. 1**, in terms of ΔT_{adia} all the irradiated samples are equivalent, when assessed in term of the efficiency upper bound calculated form **Equation. (1)**, differences become apparent. For instance, the terpo- UV- 5 min showing a relevant ΔT_{adia} improvement has a maximum efficiency drastically reduced, due to the relevant dielectric losses, getting even lower than the one of the pristine samples. Indeed, conduction losses are often present with a detrimental impact on efficiency particularly when operating at 1 Hz. **Figure. 2** shows that, using η as a figure of merit, the 20 minutes irradiated film emerges as the best refrigerant with an efficiency improvement of the order of ~80% with respect to the pristine one.

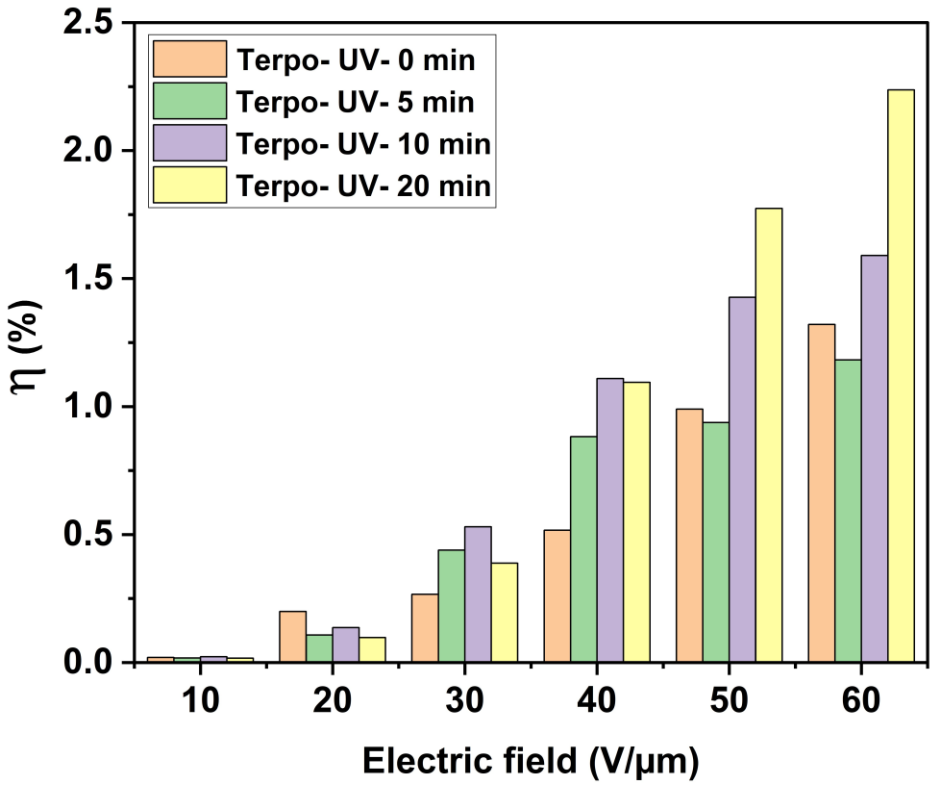

Figure. 2. Maximum relative efficiency computed from equation (2) for film with different irradiation time.

Figure. 3 shows the polarization versus electric field curve at room temperature for the pristine and irradiated terpolymer. The maximum polarization (P_{max}) is significantly increased after UV irradiation, rising from 27 mC/m^2 to 37 mC/m^2 after 20 minutes of UV exposure. The resulting higher polarization entails a higher energy storage capability. It is worth noting that all the samples exhibit the same remanence P_r, and a P_{max} increasing monotonically as a function of the irradiation time, whereas ΔT_{adia} is the same for all the irradiated films. Moreover, under 1 Hz square excitation, which corresponds to the typical device operating condition, losses increase as a function of the irradiation time up to a maximum, for the 10 minutes irradiated sample. Eventually they sharply decrease getting, for the 20 minutes irradiated film, to values close to the ones of the pristine sample Error! Reference source not found..

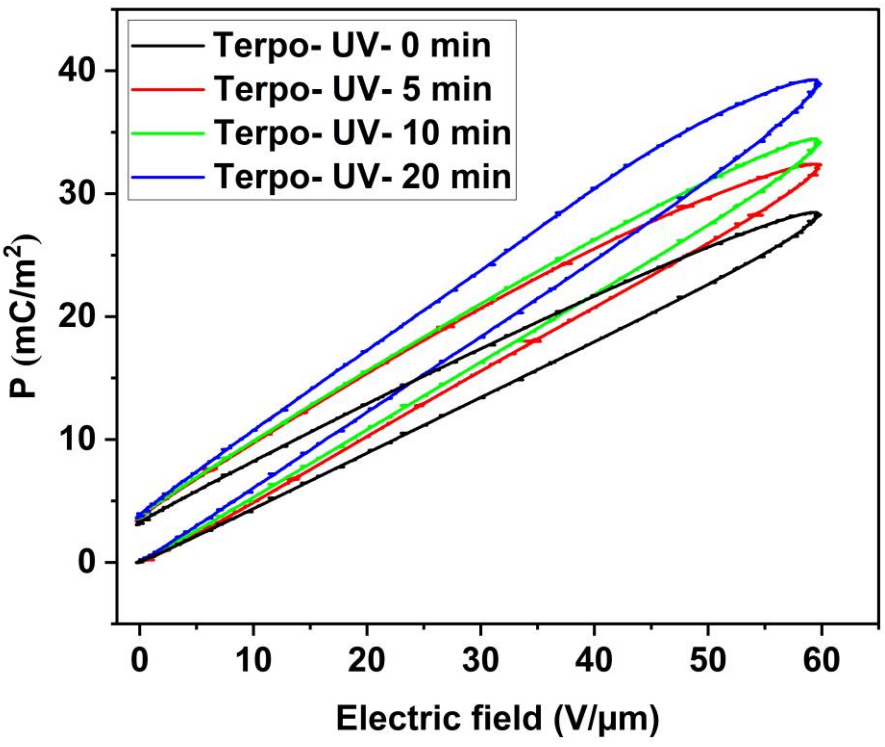

Figure. 3. Polarization versus electric field measured at 1Hz using sinus signal (working frequency of cooling device)

1. Fostering structural change under field by UV irradiation

X-Ray diffraction scan (10 °– 50 °) has been conducted on the irradiated and non-irradiated films to identify peaks corresponding to crystallinity **(**Error! Reference source not found.**)**. The peak within the 17.5 °θ – 21 °θ range is a signature of the emergence of the crystalline phase. To get an insight into the mechanism leading to EC effect enhancement presented in the previous section, X-ray diffraction (XRD) measurements under application of an electric field have been performed on the pristine and on the 20-minute irradiated terpolymers (see supplementary schematic 1). **Figure. 4** shows that the electric field induces a structural change, as indicated by the arrows, and this effect is further enhanced in the irradiated film. At high field the pic around 18.5° shows two bumps indicating two phases that are very close in their lattice parameter.

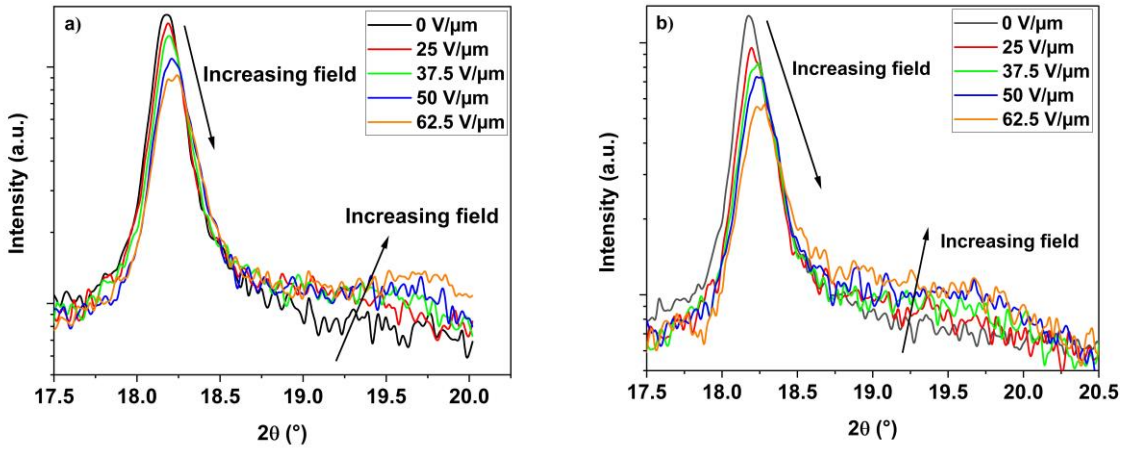

Figure. 4. X-ray spectrum with intensity in logarithmic scale, for different fields on the pristine film (on frame a) and 20 minutes irradiated film (on frame b) at 25°C.

The deconvolution of X-ray spectra, shown in the inset of **Figure.** 5 reveals three crystalline phases [28,30]. The relaxor ferroelectric phase (RFE) containing a higher number of trans *gauche* defects (tg^+tg^-) in its structure where the stacking of (tg+tg-) chains results in a significant interplanar distance, and in a characteristic peak at low 2θ; the ferroelectric phase (FE) where the chains are arranged in all-*trans* conformation resulting in a phase showing a denser crystalline structure, a lower interplanar distance and higher 2θ values; and eventually, lying between the RFE and the FE in the X-ray spectrum, the phase commonly referred to as defective ferroelectric (DFE), exhibiting an intermediate amount of (tg^+tg^-). The volume fraction of the three phases under different applied electric fields has been extracted by integration of the respective XRD spectra peaks as shown in the inset of **Figure.** 5. The phase fraction evolution as a function of the electric field is shown in **Figure.** 5 and their respective interplanar distances are shown in Table S2 (see supplementary). The subtle balance between the fractions of the three phases as a function of the electric field is the very heart of the physical mechanism underlying the EC effect.

In **Figure.** 5 the phase fractions as a function of the electric field exhibit distinct evolutions between the pristine polymer and the irradiated one. In the pristine film a slight increasing of the DFE phase over the RFE one, as a function of the field, is followed by a marginal appearance of the FE phase between 50 V/µm and 62.5 V/µm (i.e. from 0 % to less than 10 %). In the irradiated film, while the trend till 37.5 V/µm is similar, the DFE phase fraction stays almost constant between 37.5 V/µm and 62.5 V/µm while the main part of the transition takes place between 37.5 V/µm and 62.5 V/µm through the appearance of the FE phase that passes from almost 0 % up to more than 20 %. Surprisingly enough, the slight increase of the relative fraction of the DFE phase in the irradiated sample at low field seems to promote, at higher field,

the appearance of the FE phase. A similar effect has also been reported in samples treated with a method based on chemical modification [12]. The observed enhancement of the EC effect shows that the RFE to FE phase change induced by the electric field involves a higher entropy change than the RFE to DFE phase transformation.

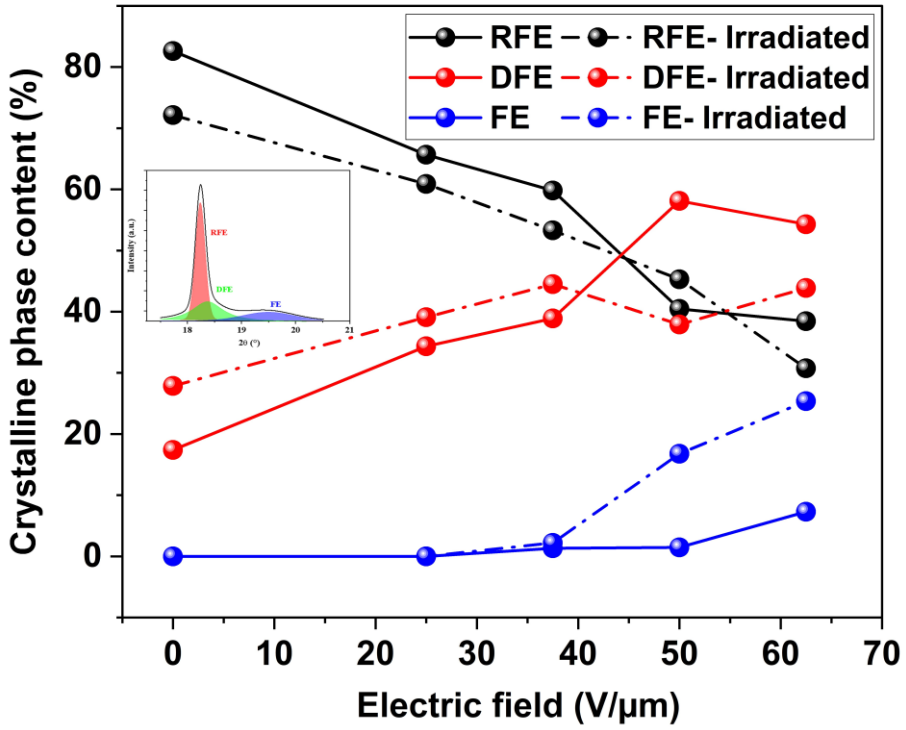

Figure. 5. Crystalline phase content in pristine terpolymer and irradiated terpolymer with 20 min UV and at 25°C.

The $\Delta T_{adia}(E)$ on **Figure. 1** and the phase fraction change under field shown on **Figure. 5**, give an insight into the relationship between change of phase and ΔT_{adia}. As expected, the ΔT_{adia} is related to the grow of the DFE or of the FE phases. At low fields ($\leq$ 20 V/μm), the transition from RFE phase to a defective ferroelectric state (DFE) in both films (irradiated and the non-irradiated) is similar and results in a small and similar ΔT_{adia} (**Figure. 1**). In this region the electric field is unable to trigger the FE phase.

Then in the irradiated films, the electric field trigger earlier the FE phase giving a higher response.

The dependence of ΔT_{adia} over the fraction of phase change is suitably described through a linear fit when assuming the entropy change associated with the RFE to FE transition to be twice the one due to the RFE to the DFE one (Error! Reference source not found.). Thence, we can expect the entropy difference between the RFE and the FE phase to be twice the one between the RFE and the DFE phases as schematically shown in **Figure. 6**.

In a simple picture (**Figure. 6**), the phase RFE are mostly related to the tg conformation, the DFE to the tttg conformation and the FE to all trans-conformation. Indeed, the RFE to FE transformation entails two times more conformation changes than the DFE to FE one, leading to an enhanced caloric effect.

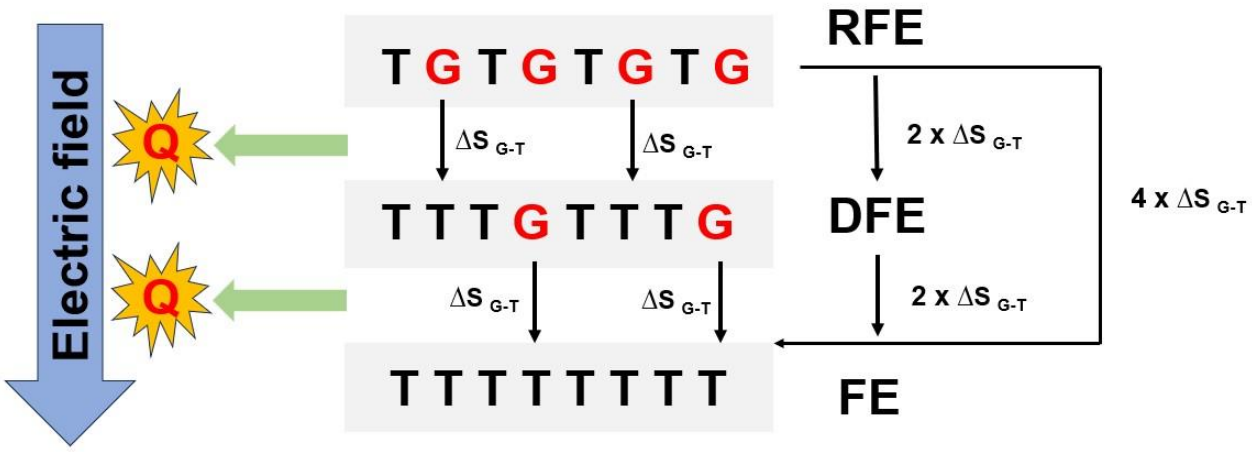

Figure. 6. Explanatory diagram of the change in conformation of the chain of the terpolymer under the application of the electric field.

Figure. 7 shows the temperature change resulting from the EC effect of pristine and irradiated films, measured at different temperatures and under different electric fields.

At low field the irradiated and the pristine film have similar temperature dependence. However, at high field with the appearance of the FE phase, as indicated in the XRD at 25°C (**Figure. 5**), the adiabatic temperature change maximum of the irradiated films shows a shift of 20°C towards higher temperatures.

Comparison between **Figure. 5** and **Figure. 6** suggests a direct relation between the lower, and higher temperature maxima with the RFE-DFE, and RFE-FE transitions respectively. A similar shift has been observed at higher applied fields on some non-modified ter-polymers able to withstand up to 100 V/μm. Unfortunately, due to the limited number of UV irradiated sample it has been impossible, so far, to explore them at field intensities where the risk of breakdown are rather important.

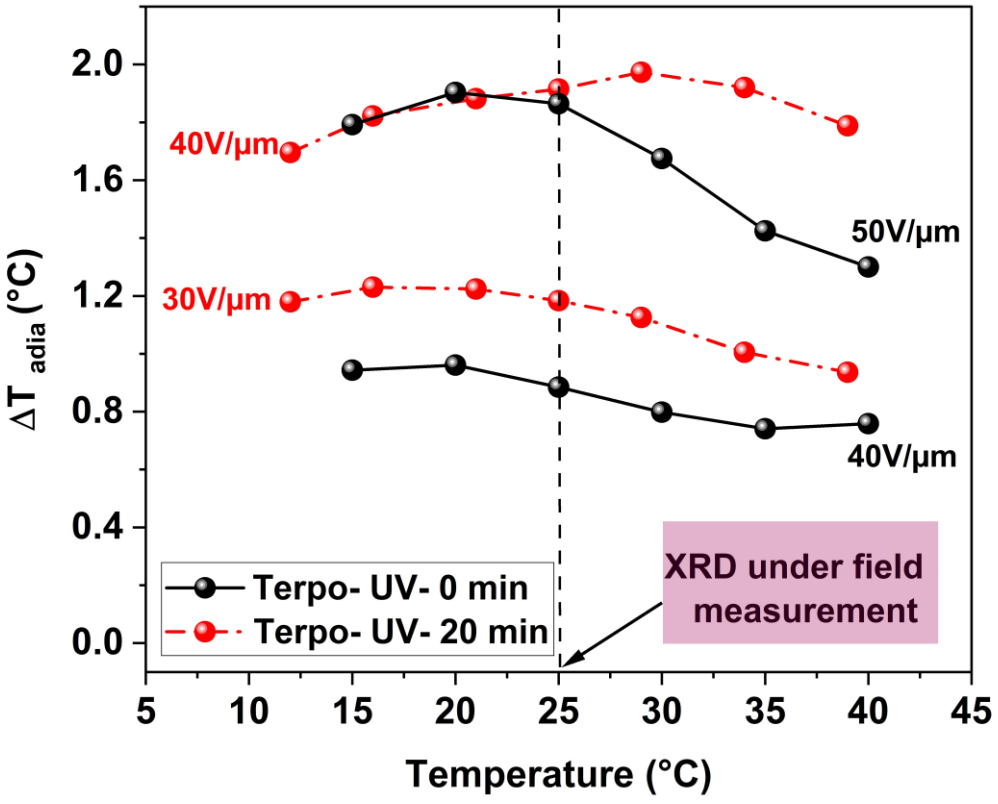

Figure. 7. Adiabatic temperature change of the pristine film and the film irradiated 20 minutes at different temperature and different field. For the Terp-UV 20 min, the field is 30, 40 V/µm and for the Terpo-UV 0min the field is 40, 50 V/µm.

2. Modification induced by UV.

To understand why a relatively low UV irradiation dose (20 minutes at 0.5 Watt) induces such a significant effect on the field driven transition, DSC measurements have been carried out. The thermal transitions of pristine and irradiated terpolymers, have been examined by differential scanning calorimetry (DSC) (Error! Reference source not found.). **Figure. 8** shows the heat flow from 45°C to 180 °C for the pristine and the 20 min irradiated terpolymer. Pristine terpolymer shows a main peak at high temperature (~128.5 °C), which is associated to the melting process. The values for the melting and Curie transitions of the samples, along with the corresponding enthalpy values and calculated crystallinities, are presented in **Table 1.** It is shown that the crystallinity (χ_c) increases with irradiation time from 30% at 0 min irradiation to 35.8% under 20 min irradiation. Indeed, the expected molecular chain cleavage of the UV, as demonstrated in PVDF alone, amplifies the degree of crystallinity within the terpolymer films. The melting point (T_m) also gradually increases with irradiation time (as shown in **Table 1**). Additionally, T_m exhibits significant broadening and a notable decrease in intensity with longer exposure time. These increases in the melting point from 128.5°C to 130°C, can be related to a lamellar thickening via the Gibbs-Thomson mechanism. We can explain this effect by the fact that UV exposure may result in the scission or breaking of polymer chains. This can create shorter chains with increased mobility, allowing them to rearrange more effectively, and leading to thicker lamellae.

In addition, the broadening is an indication of a wider crystal size distribution which can result from UV induced random chain-scission**.** A low rate of crosslinking is not

excluded because of the reactivity of the radicals formed by irradiation. Enhanced EC properties can be also partially related to this increasing of crystallinity. A closer look at the low temperature of the DSC thermograms on cooling (Figure. S6.b) shows the presence of low temperature transition around 60°C, which correspond to RFE/DFE to PE ($T_{RFE/DFE - PE}$) transition. This confirms the result found in X-ray Diffraction (XRD), which shows the presence of phases RFE /DFE at zero field (Figure 4).

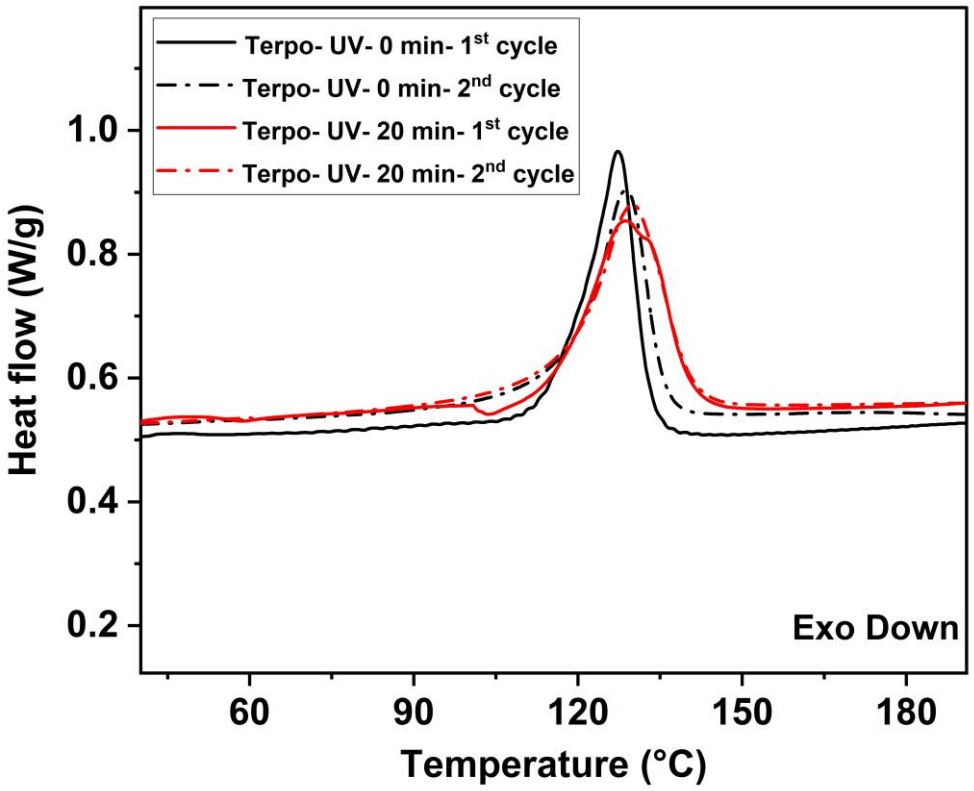

Figure. 8. Endothermic peak of melting for pristine and irradiated terpolymer. The heating rate was 20 °C/min for all samples.

Table 1. FE-PE Temperatures, Melting Temperatures, Enthalpies, and Crystallinity of pristine and irradiated terpolymer.

Sample	$T_{RFE/DFE-PE}$ [a] (°C)	T_{cryst} (°C)	T_{melt} (°C)	ΔH_{melt} (J/g)	Crystallinity DSC [b] (%)	Crystallinity XRD (%)

Terpo-UV- 0 min	62.4	94.01	128.5	12.44	30	34
Terpo-UV- 5 min	62.7	92.3	131.18	13.99	33	34
Terpo- UV- 10 min	63	92.37	130.5	15.23	36	35
Terpo- UV- 20 min	63	92.47	130.07	15.05	35.8	37

[a] DSC Curve (Figure S6. b)

[b] Cristallinity determined from $\Delta H_f^{\circ} = 42 J/g$ [31]

Fourier transform infrared spectroscopy (FTIR) has been used to inspect molecular structure before and after UV irradiation (Error! Reference source not found.). After normalizing all spectra, we plotted the relative peak intensities that are strictly related to the terpolymer structure. Comparison between the peak relative intensities before and after irradiation are shown in **Figure. 9.** A sharp intensity increase at 1736 cm^{-1} accompanied by a decrease at 1260 cm^{-1} are observed. These two peaks correspond to the CF=O (new function) and C-F bands, respectively. Besides, the bands corresponding to CH_2 and CH_3 at 2925 cm^{-1} and 2850 cm-1 respectively undergo the same variation hinting at a molecular rearrangement induced by UV exposure. The emergence of a new function (CF=O) in the IR spectrum of P(VDF-TrFE-CFE) is an indicator of polymer chain cleavage and scission. Various studies in the literature demonstrate the formation of a radical on the polymer chain because of cleavage. This active radical will capture oxygen from the air to form the CF=O functionality[23]. This compellingly suggests that UV irradiation serves as a straightforward method to modify the structure thereby augmenting the electrocaloric effect.

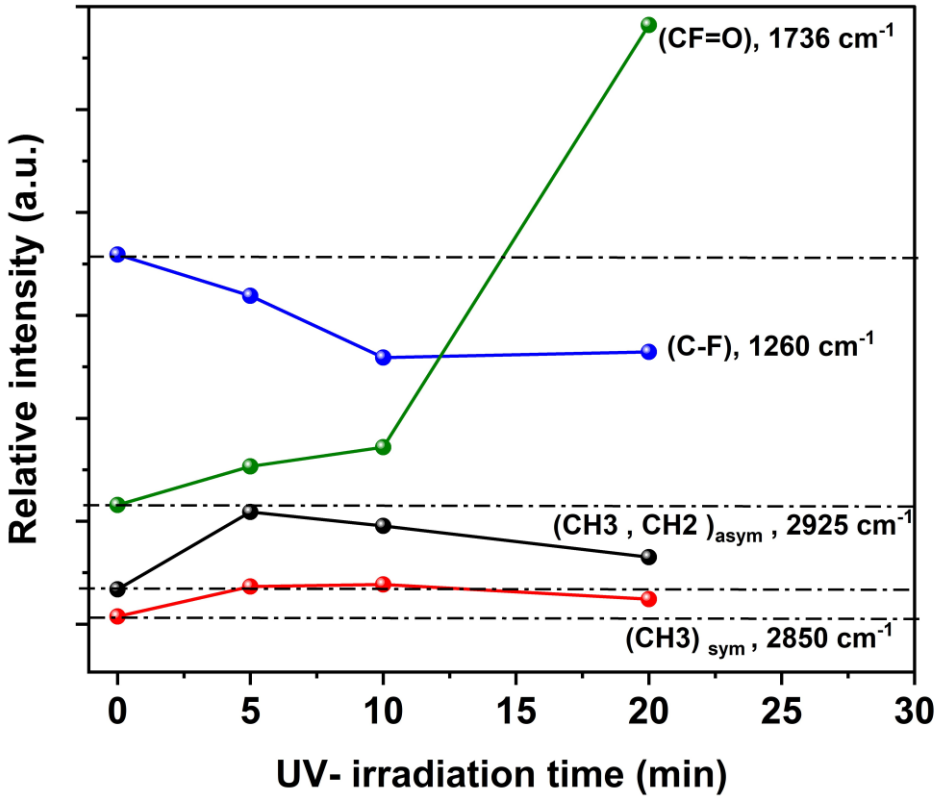

Figure. 9. Relative change in peak intensities of the CH_3 , CH_2 , C-F and CF=O bands as a function of irradiation times.

The thermal stability of the pristine and irradiated P(VDF-TrFE-CFE) films was studied by thermogravimetric analysis (TGA). The degradation temperatures are; 503 °C, 504 °C, 504.8 °C for 5, 10, and 20 min respectively. Small crosslinking effects can contribute to the thermal stability of terpolymer and cause the increasing of the decomposition temperature of PVDF [32].

III. Conclusions

In summary, our study demonstrates low-energy UV-A as an effective road to enhance the electrocaloric performance of P(VDF-TrFE-CFE), and to jointly reduce the losses

exhibited by the material under relevant working conditions. After UV-A irradiation a remarkable increase in the adiabatic temperature change, rising from 1.76°C up to 2.88°C at a field of 60 V/µm, and a significant loss reduction have been observed. This allows to estimate a ~80% enhancement of the maximum relative efficiency achievable when using the polymer as a refrigerant in a cooling device. To gain insights into the mechanisms responsible for the mentioned modifications the P(VDF-TrFE-CFE) films have been studied by XRD under applied electric field, and their adiabatic temperature change has been directly measured. Three phases have been detected, RFE, DFE, and FE. Their interplay as a function of field and temperature has been studied comparing pristine samples with the irradiated ones. After irradiation the balance between the RFE, the DFE, and the FE changes. Indeed, while the caloric effect in pristine samples is driven mainly by the RFE-DFE transition, at high filed (>40V/µm) the irradiated samples behavior is dominated by the high entropy RFE-FE transition involving a relevant EC effect enhancement.

Further investigations like GPC or AFM(-IR) are still needed to pinpoint in more detail the mechanisms responsible for the observed modifications.

The primary finding presented here is twofold: on the one hand low-energy UV-A irradiation is shown to be a road to enhance EC effect in P(VDF-TrFE-CFE) films. On the other, we show that the initial enhancement of the EC effect (up to 10 minutes irradiation time) is accompanied by a detrimental increasing of the dielectric losses in the material. Longer irradiation (up to 20 minutes) induces further structural modifications (e.g. appearance of new functional groups like CF=O or increased presence of crosslinking) bringing losses back to their initial value and making the resulting material an excellent candidate as a refrigerant for advanced solid-state refrigeration devices.

IV. Experimental

Polymer films are prepared using solution casting method, which involves dissolving P(VDF-TrFE-CFE) terpolymer powder in DMF solvent at a concentration of 10 %wt. This terpolymer contains 66.4 % VDF, 24.5% TrFE, and 9.1% CFE, expressed as molar fraction and purchased from Piezotech®. The dissolution temperature was set at 50°C, and the solution was agitated for 3 hours to achieve thermodynamic equilibrium. The resulting polymeric solution is then cast onto a clean glass plate using a calibrated casting-knife, resulting in a film with a thickness of around 14 µm ± 1 µm. To control the deposition environment condition, the coater is enclosed in a PMMA® box. The interior was purged with nitrogen for approximately twenty minutes to remove air and humidity. PVDF casting is indeed very sensitive to humidity [33] . At the time of deposition, the flow of nitrogen is stopped. After casting the glass plate is left on the plate at 30℃ for 60 minutes to form a film. After that the film is heated at 60 °C for 24 h to remove any remaining solvent. The film is then peeled off and subjected to thermal annealing at 102 ℃ to promote crystallinity.

Both sides of the terpolymer films have been exposed to UV-A at room temperature, for 5-20 minutes with an irradiance of 0.5 W/cm^2. UV irradiation was performed using a lamp of 395 nm (FluoTechnik). The radiation source was placed at 4 cm from the terpolymer films. To investigate the effect of UV irradiation on the dielectric performance, both sides of the PVDF films were exposed to UV irradiation for 5, 10, 15, and 20 minutes, and the resulting samples were labeled as Terpo-UV-5 min, Terpo-UV-10 min, and Terpo-UV-20 min, respectively. The reference sample, without irradiation is named Terpo-UV-0 min.

The crystal structure of the PVDF film was analyzed using X-ray diffraction (XRD) with Cu Kα radiation, performed on a Rigaku SmartLab instrument. X-ray under electric field were performed with a homemade diffractometer (radius = 500 mm) [34] associated with

a Rigaku RA-HF18 rotating anode generator (50 kV, 200 mA). The wavelength is copper Kalpha (1.541 A°). A nickel filter is used to eliminate the Kbeta component. Each data scan was recorded with a 2 Theta step of 0.02°, and a counting time of 1 second per step. Electric field was obtained with a Keithley 248 power unit. The film was placed on a PMMA support with copper tape on each side. Connected to this PMMA support are wires that help to apply tension. To link the top and bottom electrodes of the film with the PMMA support, we used double-sided carbon tape (brand). (see schematic 1 in the supplementary part). The measurements involved applying increasing electric fields before each new X-ray reading. Each measurement was taken at a constant electric field for a duration of 10 minutes.

The deconvolution and fitting of the XRD patterns were conducted using OriginLab software and the Voigt equation, respectively. The Avenberg-Languardt iteration algorithm was employed to effectively resolve overlapping peaks and enabling the clear identification of distinct crystalline phases (i.e. RFE, DFE and FE). The percentage of each phase was calculated by integrating the area under each deconvoluted peak.

DSC measurements were performed utilizing a TA Instruments model Q 20 DSC with a heating rate of 20 °C/min, ranging from 20 to 180 °C. Crystallinity is calculated from the area of the melting pic.

The values for the melting and Curie transitions of the above samples, along with the corresponding enthalpy values and calculated crystallinities, are presented in **Table 1.**

Fourier transform infrared spectroscopy (FTIR, Nicolet 6700) was performed on samples before the dielectric measurement. The data were recorded with 4 cm^{-1} resolution and 32 scans on a Bruker Vertex 70 spectrometer equipped with a detector from 4000 cm^{-1} to 700 cm^{-1} using the attenuated total reflectance (ATR) mode. To fabricate a capacitor-like structure, rounded gold electrodes measuring 1 cm in

diameter, and ~30 nm in thickness were applied to both sides of the terpolymer film. The gold deposition process employed was sputtering using the (Quorum, Q150T). The Polarization–electric field (P–E) loops were measured at 1 Hz using a current and voltage measurement. Thermogravimetric analysis (TGA) was performed using a Perkin-Elmer Pyris Diamond TG/DTA thermal analyzer, operating between 30 and 700 °C under a nitrogen atmosphere. The samples were placed in open ceramic crucibles, α Al_2O_3 pans, with a sample weight of ~6 mg. A heating rate of 20 ° C/min and a nitrogen flow of 20 $mL \cdot min^{-1}$ were used.

The EC effect was determined through the measurement of a flexible and thin thermistor's resistance in contact with the active part of the film. The thermistor, composed of an 8 µm thick polypropylene (PP) film metallized with an 8nm aluminum layer (Goodfellow, PP30-MZ-000180), underwent a modification to create a serpentine pattern in the measurement area using a fiber laser (Trotec, speedy 360 flexx). This laser was appropriately configured to selectively remove the metallization without causing damage to the PP film.

The resistance of the flexible thermistor (approximately 1 kΩ) was measured every 50 ms using a four-point probe and a digital multimeter (Keysight 34465A) with a sensitivity of 0.025 °C. The thermistor's surface area was 8 × 8 mm^2, smaller than that of the electrocaloric (EC) film (10 × 10 mm^2). Following calibration, the thermistor exhibited a linear dependence between resistance and temperature within the range of -10 °C to 60 °C, featuring a temperature coefficient of resistance of 0.2299%. Notably, thanks to the thermistor's shape, it remained unaffected by the electrocaloric material's electrostriction, as the associated deformation in the film plane is assumed anisotropic.

Due to its flexibility and to adhesion forces, the thermistor naturally spread over the electrocaloric film. The thermal contact quality between the film and the thermistor play

a crucial role in minimizing the sensor time response. To evaluate measurement reliability, a simulation was conducted using a 1D numerical model of a multilayer, (see our previous work [27]). This simulation considered variable air gaps between the thermistor and electrocaloric film, along with 2 mm air columns above and below the bilayer.

When a voltage square profile is applied to a terpolymer film, its temperature increases/decrease due to the EC effect. This response is measured by the flexible thermistor as a variation of resistance. By adjusting the voltage V, different heat values can be obtained.

All experimental details, with materials description, methods for film fabrication, detailed procedures, lists of instruments, and characterization techniques; Table of best EC performance (Table S1); Material losses (Figure S1); relationship between the EC effect and phase variations (Figure S2); Adiabatic temperature change (Figure S3); X-ray measurements (Figure S4); Schematic of X-ray diffraction (XRD) under electric field (Schematic 1); The interplanar distance calculated from the XRD (Table S2); FTIR measurements (Figure S5. a. b. c); DSC measurements (Figure S6, a, b); TGA measurements (Figure S7. a. b).

V. References

(1) *IEA (2018), The Future of Cooling, IEA, Paris https://www.iea.org/reports/the-future-of-cooling, License: CC BY 4.0*.

(2) Ma, R.; Zhang, Z.; Tong, K.; Huber, D.; Kornbluh, R.; Ju, Y. S.; Pei, Q. Highly Efficient Electrocaloric Cooling with Electrostatic Actuation. *Science (80-.).*

2017, *357* (6356), 1130–1134.

(3) Meng, Y.; Zhang, Z.; Wu, H.; Wu, R.; Wu, J.; Wang, H.; Pei, Q. A Cascade Electrocaloric Cooling Device for Large Temperature Lift. *Nat. Energy* **2020**, *5* (12), 996–1002.

(4) Bo, Y.; Zhang, Q.; Cui, H.; Wang, M.; Zhang, C.; He, W.; Fan, X.; Lv, Y.; Fu, X.; Liang, J.; Huang, Y.; Ma, R.; Chen, Y. Electrostatic Actuating Double-Unit Electrocaloric Cooling Device with High Efficiency. *Adv. Energy Mater.* **2021**, *11* (13), 1–8.

(5) Neese, B.; Lu, S. G.; Chu, B.; Zhang, Q. M. Electrocaloric Effect of the Relaxor Ferroelectric Poly(Vinylidene Fluoride-Trifluoroethylene-Chlorofluoroethylene) Terpolymer. *Appl. Phys. Lett.* **2009**, *94* (4), 042910.

(6) Ma, R.; Zhang, Z.; Tong, K.; Huber, D.; Kornbluh, R.; Ju, Y. S.; Pei, Q. Highly Efficient Electrocaloric Cooling with Electrostatic Actuation. *Science (80-.).* **2017**, *357* (6356), 1130–1134.

(7) Hu, H.; Zhang, F.; Luo, S.; Chang, W.; Yue, J.; Wang, C. H. Recent Advances in Rational Design of Polymer Nanocomposite Dielectrics for Energy Storage. *Nano Energy* **2020**, *74*, 104844..

(8) Liu, Y.; Zhang, B.; Xu, W.; Haibibu, A.; Han, Z.; Lu, W.; Bernholc, J.; Wang, Q. Chirality-Induced Relaxor Properties in Ferroelectric Polymers. *Nat. Mater.* **2020**, *19* (11), 1169–1174.

(9) Yang Liu, Haibibu Aziguli, Bing Zhang, Wenhan Xu, Wenchang Lu, J. Bernholc, Q. W. Ferroelectric Polymers Exhibiting Behaviour Reminiscent of a Morphotropic Phase Boundary. *Nat. Lett.* **2018**, *562* (7725).

(10) Bao, H.; Song, J.; Zhang, J.; Shen, Q.; Yang, C.; December, R. V; Re, V.; Recei, M.; February, V. Phase Transitions and Ferroelectric Relaxor Behavior in P (VDF - TrFE - CFE) Terpolymers. *Macromelecules* **2007**, *40* (7), 2371–2379.

(11) Yang, L.; Tyburski, B. A.; Domingues, F.; Santos, D.; Endoh, M. K.; Koga, T.; Huang, D.; Wang, Y.; Zhu, L.; Piezotech, S. A. S.; Moissan, R. H. Relaxor Ferroelectric Behavior from Strong Physical Pinning in a Poly(Vinylidene Fl Uoride- Co -Tri Fl Uoroethylene- Co - Chlorotri Fl Uoroethylene) Random Terpolymer. **2014**, *47* (22), 8119–8125.

(12) Qian, X.; Han, D.; Zheng, L.; Chen, J.; Tyagi, M.; Li, Q.; Du, F.; Zheng, S.; Huang, X.; Zhang, S.; Shi, J.; Huang, H.; Shi, X.; Chen, J.; Qin, H.; Bernholc, J.; Chen, X.; Chen, L. Q.; Hong, L.; Zhang, Q. M. High-Entropy Polymer Produces a Giant Electrocaloric Effect at Low Fields. *Nature* **2021**, *600* (7890), 664–669.

(13) Chen, Y.; Qian, J.; Yu, J.; Guo, M.; Zhang, Q.; Jiang, J.; Shen, Z.; Chen, L. Q.; Shen, Y. An All-Scale Hierarchical Architecture Induces Colossal Room-Temperature Electrocaloric Effect at Ultralow Electric Field in Polymer Nanocomposites. *Adv. Mater.* **2020**, *32* (30), 1–9.

(14) Zhang, G.; Li, Q.; Gu, H.; Jiang, S.; Han, K.; Gadinski, M. R. Ferroelectric Polymer Nanocomposites for Room-Temperature Electrocaloric Refrigeration COMMUNICATION. **2015**, 1–5.

(15) Qian, J.; Peng, R.; Shen, Z.; Jiang, J.; Xue, F.; Yang, T.; Chen, L.; Shen, Y. Interfacial Coupling Boosts Giant Electrocaloric Effects in Relaxor Polymer Nanocomposites: In Situ Characterization and Phase-Field Simulation. *Adv. Mater.* **2019**, *31* (5), 1–9.

(16) Hassan, Y. A.; Chen, L.; Geng, X.; Jiang, Z.; Zhang, F.; Luo, S.; Hailong Hu. Electrocaloric Effect of Structural Configurated Ferroelectric Polymer Nanocomposites for Solid-State Refrigeration. *ACS Appl. Mater. Interfaces* **2021**, *13* (39), 46681–46693.

(17) Goupil, F. Le; Kallitsis, K.; Tencé-girault, S.; Brochon, C.; Cloutet, E.; Soulestin, T.; Santos, D.; Stingelin, N.; Hadziioannou, G.; Goupil, F. Le; Kallitsis, K.; Tencé-

girault, S.; Pouriamanesh, N.; Brochon, C. Enhanced Electrocaloric Response of Vinylidene Fluoride – Based Polymers via One-Step Molecular Engineering. *Adv. Funct. Mater.* **2020**, *31* (1), 2007043.

(18) Kang, L.; Hong, L.; Zheng, L.; Qian, X. Statistical Mechanical Model of the Giant Electrocaloric Effect in Ferroelectric Polymers. *ACS macro Lett.* **2023**, *12*, 848–853.

(19) A.M. Guzman, J.D. Carlson, J.E. Bares, P. P. P. Chemical and Physical Changes Induced in Polyvinylidene Fluoride by Irradiation with High Energy Ions. *Nucl. Instruments Methods Phys. Res. B* **1985**, *8*, 468–472.

(20) Yang, L.; Li, X.; Allahyarov, E.; Taylor, P. L.; Zhang, Q. M.; Zhu, L. Novel Polymer Ferroelectric Behavior via Crystal Isomorphism and the Nanoconfinement Effect Novel Polymer Ferroelectric Behavior via Crystal Isomorphism and the Nanocon Fi Nement Effect. *Polymer (Guildf).* **2013**, *54* (7), 1709–1728.

(21) Rosenberg, Y.; Siegmann, A.; Narkis, M.; Shkolnik, S. The Sol/Gel Contribution to the Behavior of Γ-irradiated Poly(Vinylidene Fluoride). *J. Appl. Polym. Sci.* **1991**, *43* (3), 535–541. https://doi.org/10.1002/app.1991.070430314.

(22) Holland, F. A. Kirk-Othmer Encyclopedia of Chemical Technology. *Endeavour*. 1978, p 193.

(23) Katan, E.; Narkis, M.; Siegmann, A. The Effect of Some Fluoropolymers' Structures on Their Response to UV Irradiation. *J. Appl. Polym. Sci.* **1998**, *70* (8), 1471–1481.

(24) Liu, H.; Li, B. W.; Chen, J.; Shen, Z.; Zhang, X.; Wang, J.; Nan, C. W. Concurrent Enhancement of Breakdown Strength and Dielectric Constant in Poly(Vinylidene Fluoride) Film with High Energy Storage Density by Ultraviolet Irradiation. *ACS Omega* **2022**, *7* (30), 25999–26004.

(25) Botelho, G.; Silva, M. M.; Gonçalves, A. M.; Sencadas, V.; Serrado-nunes, J.;

Lanceros-mendez, S. Performance of Electroactive Poly (Vinylidene Fluoride) against UV Radiation. **2008**, *27*, 818–822.

(26) Berthelot, T.; Tuan, X.; Jégou, P.; Viel, P.; Boizot, B.; Baudin, C.; Palacin, S. Applied Surface Science Photoactivated Surface Grafting from PVDF Surfaces. *Appl. Surf. Sci.* **2011**, *257* (22), 9473–9479.

(27) Zeggai, N.; Dkhil, B.; Lobue, M.; Almanza, M. Cooling Efficiency and Losses in Electrocaloric Materials. *Appl. Phys. Lett.* **2023**, *122* (8), 081903.

(28) Goupil, F. Le; Coin, F.; Pouriamanesh, N.; Fleury, G. Electrocaloric Enhancement Induced by Cocrystallization of Vinylidene Difluoride-Based Polymer Blends . **2021**, *10* (12), 1555–1562.

(29) Qian, X.; Han, D.; Zheng, L.; Chen, J.; Tyagi, M.; Li, Q.; Du, F.; Zheng, S.; Huang, X.; Zhang, S.; Shi, J.; Huang, H.; Shi, X.; Chen, J.; Qin, H.; Bernholc, J.; Chen, X.; Chen, L. Q.; Hong, L.; Zhang, Q. M. High-Entropy Polymer Produces a Giant Electrocaloric Effect at Low Fields. *Nature* **2021**, *600* (7890), 664–669.

(30) Bargain, F.; Thuau, D.; Hadziioannou, G.; Domingues, F.; Santos, D.; Tenc, S. Phase Diagram of Poly (VDF- Ter -TrFE- Ter -CTFE) Copolymers : Relationship between Crystalline Structure and Material Properties. *Polymer (Guildf).* **2020**, *2013*, 123203.

(31) Klein, R. J.; Runt, J.; Zhang, Q. M. Influence of Crystallization Conditions on the Microstructure and Electromechanical Properties of Poly (Vinylidene Fluoride - Trifluoroethylene - Chlorofluoroethylene) Terpolymers. *Macromolecules* **2003**, *36* (19), 7220–7226.

(32) Jaleh, B.; Gavary, N.; Fakhri, P.; Muensit, N.; Taheri, S. M. Characteristics of PVDF Membranes Irradiated by Electron Beam. *Membranes (Basel).* **2015**, *5* (1), 1–10.

(33) Li, M.; Katsouras, I.; Piliego, C.; Glasser, G.; Lieberwirth, I.; Blom, P. W. M.; De

Leeuw, D. M. Controlling the Microstructure of Poly(Vinylidene-Fluoride) (PVDF) Thin Films for Microelectronics. *J. Mater. Chem. C* **2013**, *1* (46), 7695–7702.

(34) J. F. BERAR, G. C. E. D. W. Un Goniomètre Original Très Précis Pour La Diffraction Des Rayons X Sur Poudre à Température Controlée. *J. Appl. Crystallogr.* **1980**, *13*, 201–206.

VI. Acknowledgements

The authors declare that they do not have any known competing financial interests or personal relationships that could have appeared to influence the work reported in this paper. This work has benefited from the financial support of the LabEx LaSIPS (ANR-10-LABX-0032-LaSIPS) under the "Investissements d'avenir" program (ANR-11-IDEX-0003) and from (ANR-20-CE05-0044), which are both managed by the French National Research Agency.